



# Mitochondrial outer membrane permeabilization and inner membrane permeabilization in regulating apoptosis and inflammation

Hong Qi<sup>a,b,\*</sup>, Yu-Song Yin<sup>a</sup>, Zhi-Yong Yin<sup>c</sup>, Xiang Li<sup>d</sup>, Jian-Wei Shuai<sup>b</sup>

<sup>a</sup> Complex Systems Research Center, Shanxi University, Taiyuan, China

<sup>b</sup> Wenzhou Key Laboratory of Biophysics, Wenzhou Institute, University of Chinese Academy of Sciences, Wenzhou, China

<sup>c</sup> School of Mathematics and Statistics, Guangxi Normal University, Guilin, China

<sup>d</sup> Department of Physics and Fujian Provincial Key Laboratory for Soft Functional Materials Research, Xiamen University, Xiamen, China

## ARTICLE INFO

### Keywords:

Mitochondrial outer membrane permeabilization  
Mitochondrial inner membrane permeabilization  
Apoptosis  
Inflammation  
Dynamic mechanism

## ABSTRACT

Recent studies delineate an intimate crosstalk between apoptosis and inflammation. However, the dynamic mechanism linking them by mitochondrial membrane permeabilization remains elusive. Here, we construct a mathematical model consisting of four functional modules. Bifurcation analysis reveals that bistability stems from Bcl-2 family member interaction and time series shows that the time difference between Cyt c and mtDNA release is around 30 min, which are consistent with previous works. The model predicts that Bax aggregation kinetic determines cells to undergo apoptosis or inflammation, and that modulating the inhibitory effect of caspase 3 on IFN- $\beta$  production allows the concurrent occurrence of apoptosis and inflammation. This work provides a theoretical framework for exploring the mechanism of mitochondrial membrane permeabilization in controlling cell fate.

## 1. Introduction

It has been long established that proteins of Bcl-2 family are critical players in the mitochondrial pathway leading to apoptosis (Youle and Strasser, 2008), an immunologically silent form of cell death (Bedoui et al., 2020). These proteins form a complex interaction network that controls mitochondrial outer membrane permeabilization (MOMP) and the subsequent release of cytochrome c (Cyt c), which mediates the activation of caspase 3 (Ow et al., 2008), a key and often defining event in the process of apoptosis (Fox and Aubert, 2008). According to their role in influencing the occurrence of MOMP and consequent apoptosis, Bcl-2 family members are categorized into three groups (Czabotar et al., 2014; Youle and Strasser, 2008). The proapoptotic effectors, including Bak and Bax, when activated, oligomerize and form pores in the membrane, causing MOMP. Active effectors are bound and inhibited by guardians, such as Bcl-2 and Bcl-x<sub>L</sub>, thereby blocking apoptosis. The third class that called initiators, such as Bid, Bim and Bad, sense diverse apoptotic stimuli and initiate apoptosis. The initiators can be further classified into two subgroups: the sensitizers (Bad) function only to antagonize the guardians, whereas the activators (Bid and Bim) can directly activate the effectors in addition to suppressing the guardians (Green and Levine, 2014; Singh et al., 2019).

A recent and important study showed that the effectors Bax/Bak are not only responsible for the MOMP-mediated efflux of Cyt c and consequent activation of caspase 3, but also provide a gateway for mitochondrial inner membrane permeabilization (MIMP), allowing mitochondrial DNA (mtDNA) to be exposed to the cytosol (McArthur et al., 2018). On entering the cytosol, mtDNA engages the cGAS-STING signaling pathway that culminates in the synthesis of interferon- $\beta$  (IFN- $\beta$ ), which is involved in innate immune responses and inflammation (Cosentino and García-Sáez, 2018; Riley et al., 2018). Notably, activated caspase 3 attenuates this mtDNA-induced cGAS-STING pathway, thus maintaining apoptosis immunologically silent (Ning et al., 2019; Rongvaux et al., 2014; White et al., 2014).

Although the above-mentioned experimental results (McArthur et al., 2018; Riley et al., 2018) revealed that the effectors Bax/Bak operate, through MOMP and MIMP, at the interface between apoptosis and inflammation (Cosentino and García-Sáez, 2018; Galluzzi and Vanpouille-Box, 2018), the dynamic mechanism linking apoptosis and inflammation remains enigmatic. Considering the fact that active Bax can form pores of variable size (Große et al., 2016; Salvador-Gallego et al., 2016), we hypothesized that low-order oligomers of Bax induce the formation of MOMP that liberates Cyt c and initiates apoptosis, while high-order oligomers facilitate the occurrence of MIMP that releases

\* Corresponding author.

E-mail address: [hongqi@sxu.edu.cn](mailto:hongqi@sxu.edu.cn) (H. Qi).

mtDNA and triggers inflammation. That is to say, the kinetics of oligomeric state of Bax is critical for mitochondrial content release, and hence for determination of different cell fates.

Taking this hypothesis into account, we constructed a mathematical model, which is based on our previous model (Yin et al., 2017) as well as incorporates another relevant model (Kueh et al., 2016) and some recent related experimental findings (McArthur et al., 2018; Ning et al., 2019; Riley et al., 2018). As a result, the present model consists of four modules: Bcl-2 family members' interaction, assembly of MOMP and MIMP, Cyt c-induced caspase 3 activation, and mtDNA-driven IFN- $\beta$  production. Bifurcation analysis demonstrates that the bistable behavior is obtained in the first module. Time series analysis shows that the time difference between Cyt c and mtDNA release is around 30 min. These two simulation results are consistent with previous theoretical and experimental results. The model also makes several compelling predictions about how to control cell fate. Especially, the aggregation kinetic of Bax oligomers plays a crucial role in the decision of apoptosis or inflammation. Unexpectedly, manipulating the inhibitory effect of caspase 3 on IFN- $\beta$  production can allow apoptosis and inflammation to occur simultaneously. Hence, this work provides a theoretical framework for studying the dynamical mechanism linking apoptosis and inflammation and advances the understanding of mitochondrial membrane permeabilization in controlling cell fate.

## 2. Model and method

### 2.1. Model description

Mitochondria are crucial for a wide variety of cellular processes, including energy metabolism, calcium homeostasis, reactive oxygen species generation (Gutiérrez et al., 2020; Qi et al., 2020b), apoptosis, and inflammation (Fig. 1A). A healthy mitochondrion has four distinct compartments that include outer membrane, intermembrane space, inner membrane, and matrix (Pfanner et al., 2019). Cyt c and mtDNA are located in the intermembrane space and the matrix, respectively (Youle, 2019). Activation of the effectors of Bcl-2 family results in not only the occurrence of MOMP and the subsequent release of Cyt c which

eventually activates apoptotic pathway, but also the occurrence of MIMP and the consequent liberation of mtDNA which is the mediator of inflammation. To decipher the dynamic mechanism underlying these phenomena, we built a model consisting of four functional modules (Fig. 1B), which are detailed in following paragraphs.

The first module is the input module which represents the interaction between members of Bcl-2 family. To reduce the complexity, proteins with similar biological function are often represented by a single species (Albeck et al., 2008; Cui et al., 2008; Yin et al., 2017). Furthermore, the experimental result showed that although both Bid and Bim have the ability to activate both Bak and Bax, they exhibit differential preferences: Bid preferentially activates Bak, while Bim preferentially activates Bax (Sarosiak et al., 2013). As a result, we chose Bax to represent the effectors, Bcl-2 to represent the guardians, Bad to represent the sensitizers, and Bim to represent the activators. We used the unified mode, which is explained in detail in our previous paper (Yin et al., 2017), to describe the interplay between the four subgroups of Bcl-2 family. Bim and Bad are upregulated in response to cellular stress. Bim binds to Bax and converts it into activated form (AcBax), which can be inhibited by Bcl-2 via complex formation. On the other hand, Bim and Bad are able to neutralize Bcl-2.

The second module is designed to consider the relationship between MOMP and MIMP. AcBax inserts into the mitochondrial outer membrane as a monomer. Then, monomers self-assemble into oligomers, giving rise to different oligomeric species based on multiples of dimers (Subburaj et al., 2015). As done in a previous kinetic study (Kueh et al., 2016), we assumed that bigger oligomers form through successive dimerization of smaller oligomers. We further assumed that dimers (AcBax<sub>2</sub>), tetramers (AcBax<sub>4</sub>) and octamers (AcBax<sub>8</sub>) are the constituents of MOMP, while octamers, hexamers (AcBax<sub>16</sub>) and 32-mers (AcBax<sub>32</sub>) are responsible for MIMP.

The third and fourth module are the output modules, which roughly capture the profile of signaling pathway of apoptosis and inflammation, respectively. Following the occurrence of MOMP, Cyt c release from the intermembrane space that activates downstream caspase 3, thereby executing apoptosis. The macropores formed by MIMP induce the occurrence of MIMP, which allows mtDNA efflux from the matrix that

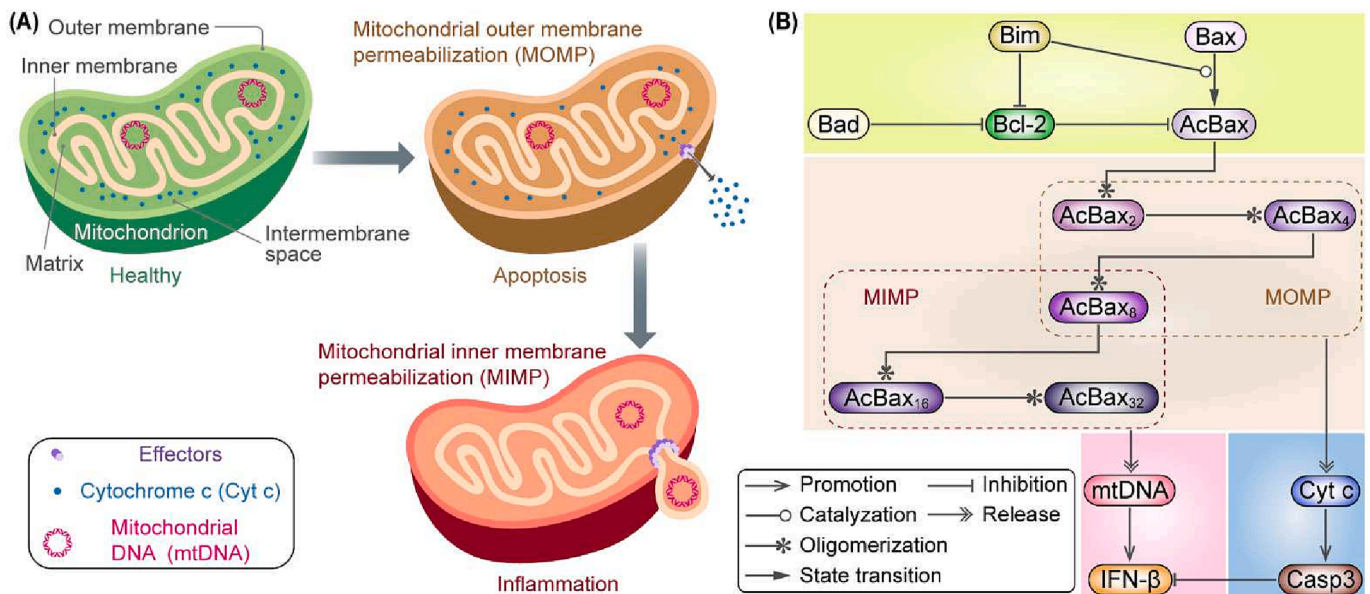


**Fig. 1.** Working hypothesis and model. (A) A mitochondrion has four parts, i.e., outer membrane, intermembrane space, inner membrane, and matrix. Under healthy condition, Cyt c is retained in the intermembrane space, and mtDNA is localized in the matrix. In the presence of apoptotic stimuli, the effectors of Bcl-2 family oligomerize in the outer membrane to form the pores responsible for MOMP, which permits the release of Cyt c. MIMP occurs with the expansion of these pores and the extrusion of the inner membrane, which enables the escape of mtDNA, thereby evoking inflammation. (B) The model comprises four modules: Bcl-2 family member interaction, MOMP and MIMP caused by different sizes of oligomers formed by activated Bax, Cyt c-induced caspase 3 activation, and mtDNA-mediated IFN- $\beta$  production, which are marked by different background colors. See more details in the main text.

drives the synthesis of IFN- $\beta$ , leading to inflammation. However, caspase 3 attenuates the inflammatory reaction by cleaving the key proteins required for IFN- $\beta$  production (Ning et al., 2019; White et al., 2014).

## 2.2. Equations and parameters

The model contains 19 components, including the different states of the same protein (e.g., Bax and AcBax), the complex formed by two distinct proteins (e.g., Bim:Bcl-2), the different oligomeric species (e.g., AcBax<sub>2</sub> and AcBax<sub>4</sub>), and the same molecule in different subcellular compartments (e.g., Cyt c in the mitochondria and in the cytosol). The physical and chemical reactions among the 19 components are translated into ordinary differential equations (ODEs). The synthesis reaction is considered only for the proteins originally present in the cell, while the degradation reaction is considered for all species. The binding and release process are described by mass action kinetics (Hantusch et al., 2018; Huber et al., 2011). Considering the fact that the pores formed by AcBax have different sizes, we assumed that the release rate of mitochondrial content (i.e., Cyt c and mtDNA) is linearly dependent on the size of the pore. Due to the multistep reactions involved in the activation of caspase 3 by Cyt c and the regulation of IFN- $\beta$  production by mtDNA and caspase 3, Hill function is employed to characterize these complex process (Qi et al., 2021; Wang et al., 2019; Zhang et al., 2011). The 19 ODEs and their associated reaction rates and synthesis-degradation rates are listed in Table S1.

Table S2 summarizes the meaning of parameters and their standard value. The geometric parameters, synthesis and degradation rates, and kinetics parameters within Bcl-2 family interaction module are from our previous studies (Qi et al., 2020a; Yin et al., 2017). The synthesis rate of mtDNA is deduced by its copy number (Frahm et al., 2005; Satoh and Kuroiwa, 1991). The dissociation rate constant of AcBax oligomers is from a relevant model (Kueh et al., 2016). The dimerization rate constant of AcBax oligomers and the release rate constant of mitochondrial content are estimated by fitting the experimental data, i.e., the release time interval between Cyt c and mtDNA is about 30 min (Cosentino and García-Sáez, 2018). The activation rate constants of caspase 3 and IFN- $\beta$  are adopted to keep their concentrations within the physiological range (Qi et al., 2020a; Wang et al., 2016). The half-saturation constants are assigned values roughly within an order of magnitude of their respective substrate concentrations.

It is important to note that the input of the model is Bim-mediated activation rate constant of Bax ( $k_1$ ), and the outputs of the model are the amounts of caspase 3 and IFN- $\beta$ , which represent apoptosis and inflammation, respectively.

## 3. Results

### 3.1. Bifurcation analysis

Previous theoretical and experimental studies showed that the complex interactions among Bcl-2 family members confer a bistable switch in the activation of Bax (Mu et al., 2021; Sun et al., 2010; Yin et al., 2017). We expected this property can be retained in the module of Bcl-2 family protein interaction, which is similar to the original model (Yin et al., 2017).

Bifurcation analysis that qualitatively captures the long-term dynamic behavior of the examined system (Frank et al., 2021), is used to demonstrate bistability. Given the biological importance of Bim-mediated Bax activation in the emergence of bistability (Yin et al., 2017),  $k_1$  is selected as the bifurcation parameter to illustrate how the system dynamics change with varying input signals. From Fig. 2 we see that all four members of Bcl-2 family as well as AcBax and its oligomers exhibit bistable dynamics (AcBax<sub>16</sub> and AcBax<sub>32</sub> are not presented due to extremely low levels of concentration).

Overall, the eight bifurcation diagrams in Fig. 2 show two different trends. Bim and Bad contribute to the activation of Bax, so they have an identical trend with AcBax and its oligomers (AcBax<sub>2</sub>, AcBax<sub>4</sub>, AcBax<sub>8</sub>), i.e., low stable steady state in smaller  $k_1$  and high stable steady state in bigger  $k_1$ . Although both Bcl-2 and Bax have an opposite trend with AcBax, the underlying mechanisms are different: Bcl-2 inhibits AcBax, and Bax converts into AcBax. Thus, the results of the bifurcation analysis are consistent with the biological relevance of these species.

### 3.2. Standard time series

Fig. 3 shows the time series of all species in the last three modules under standard parameter values. As detailed in Fig. 3A, the concentrations of AcBax, AcBax<sub>2</sub>, and AcBax<sub>4</sub> can reach tens of nanomolar, the concentration of AcBax<sub>8</sub> is at low nanomolar level, as well as the concentrations of AcBax<sub>16</sub> and AcBax<sub>32</sub> are at sub-nanomolar levels. Due to the huge difference between the amount of MOMP (including AcBax<sub>2</sub>, AcBax<sub>4</sub>, and AcBax<sub>8</sub>) and the amount of MIMP (including AcBax<sub>8</sub>, AcBax<sub>16</sub>, and AcBax<sub>32</sub>), Cyt c release precedes mtDNA release from mitochondria into the cytosol (Fig. 3B).

In order to quantitatively compare the release dynamics between Cyt c and mtDNA, we defined a time difference ( $T_d$ ) as the time required for mtDNA to reach 10% of its maximum value ( $T_{m0.1}$ ) minus the time required for Cyt c to reach 10% of its maximum value ( $T_{c0.1}$ ). As illustrated in Fig. 3B, the time difference is 33.5 min, in line with the time interval observed in experiment (Cosentino and García-Sáez, 2018).

As time progressed, Cyt c and mtDNA are all fully released into the cytoplasm, where they respectively activate caspase 3 and IFN- $\beta$

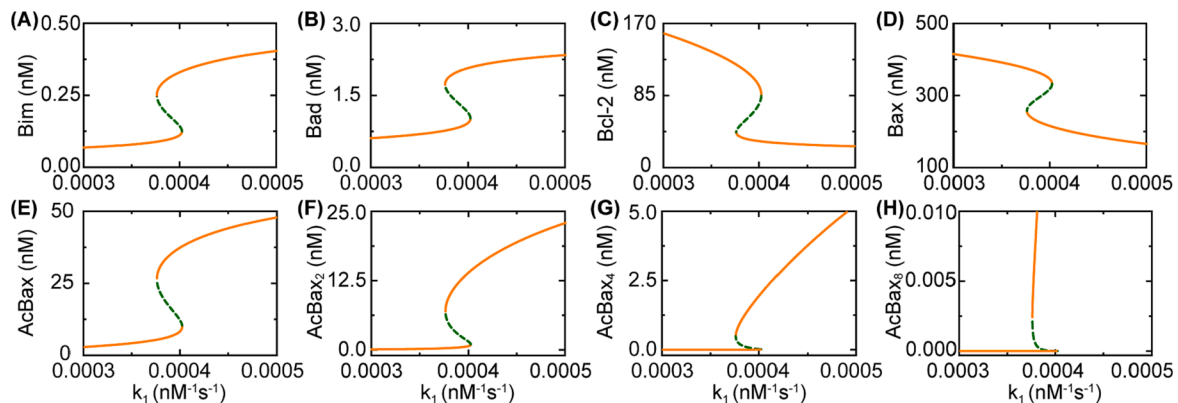
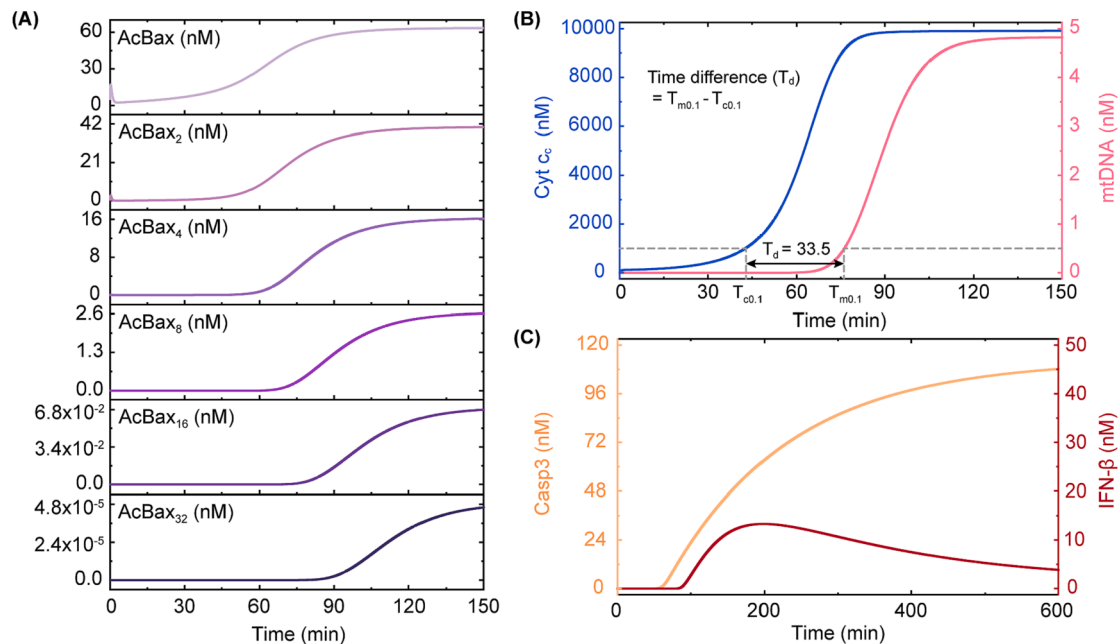


Fig. 2. The bifurcation diagrams of the Bcl-2 family members with respect to  $k_1$ , Bim-mediated activation rate constant of Bax. The solid and dashed lines denote stable and unstable steady states, respectively.



**Fig. 3.** The time courses of activated form of Bax (AcBax) and its n-order oligomers AcBax<sub>n</sub> (A), Cyt c and mtDNA in the cytosol (B), and caspase 3 and IFN-β (C) under standard parameter values. Cyt c<sub>c</sub> means the Cyt c in the cytosol.

(Fig. 3C). The activation time of caspase 3 is approximately 10 h, reflecting the typical timescale of caspase activation (Lee et al., 2010; Qi et al., 2020a). The reason why IFN-β first rises and then falls is that caspase 3 plays an inhibitory role in IFN-β production.

### 3.3. Sensitivity analysis

To investigate the impact of all the 15 parameters upstream of the release event on  $T_d$ , we performed sensitivity analysis by increasing or decreasing each parameter by 10% of its standard value while keeping the remaining parameters constant. We specified that if the percentage change of  $T_d$  exceeds 5%, it is classified as a most sensitive parameter; if the change is less than 1%, it is classified as an insensitive parameter; otherwise, it is classified as a sensitive parameter.

As depicted in Fig. 4, each of the three classes has five parameters, which are marked by light orange, green, and purple, respectively. It should be pointed out that the most sensitive parameter is  $k_1$ , meaning that it has the greatest impact on  $T_d$ , and the most insensitive parameter is the association rate constant of Bad and Bcl-2 ( $k_4$ ). Overall, the percentage change of  $T_d$  is within -11% ~ 13%. That is to say,  $T_d$  can range from 29.8 min to 37.9 min, indicating the robustness of the release event against changes in parameter values. On the other hand, all of the most

sensitive parameters are related to the first module, demonstrating the absolute control of Bcl-2 family members over the release event.

### 3.4. Influence of parameters on cell fate

In the present study, cells theoretically have three fates: undergoing apoptosis without inflammation, undergoing inflammation without apoptosis, and undergoing both apoptosis and inflammation. We next focused on analyzing whether the cell fate can be altered by a change in parameter values. Here the concentrations of caspase 3 and IFN-β at 10 h are used as the index for cell fate. By testing the 15 parameters in Fig. 4 one by one, we found that only two parameters have marked effect on cell fate transition (Fig. 5).

For the reason of space, we chose the most insensitive parameter  $k_4$  and the most sensitive parameter  $k_1$  as two examples to illustrate the scenario that most of the parameters have no substantial effect on cell fate transition. From Fig. 5A we can see that regardless of the variation in parameter  $k_4$ , the amount of caspase 3 is always high while the amount of IFN-β is always low, implying that cells always undergo apoptosis without inducing inflammation. Fig. 5B shows that when  $k_1$  exceeds a threshold value, caspase 3 is kept high while IFN-β is very low, which also means that cells involve apoptosis without provoking

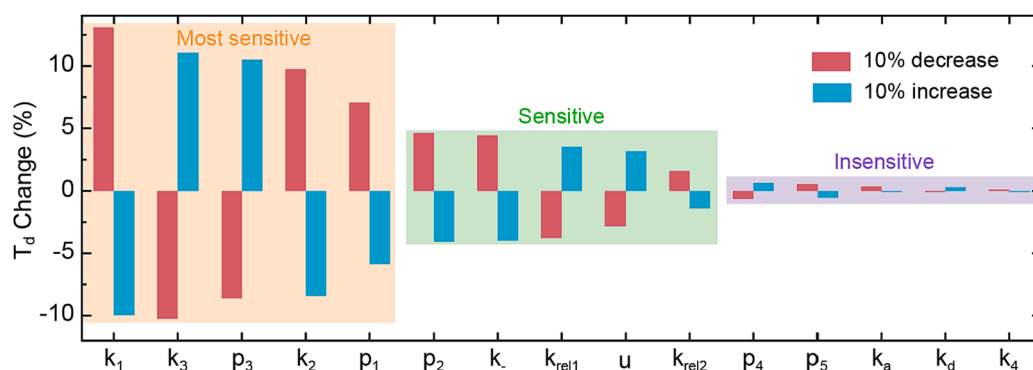


**Fig. 4.** Parameter sensitivity analysis for release time difference ( $T_d$ ) between Cyt c and mtDNA. Percentage change of  $T_d$  in response to 10% decrease (red bar) or increase (blue bar) of each parameter. The physical meanings of the 15 parameters are listed in Table S2.

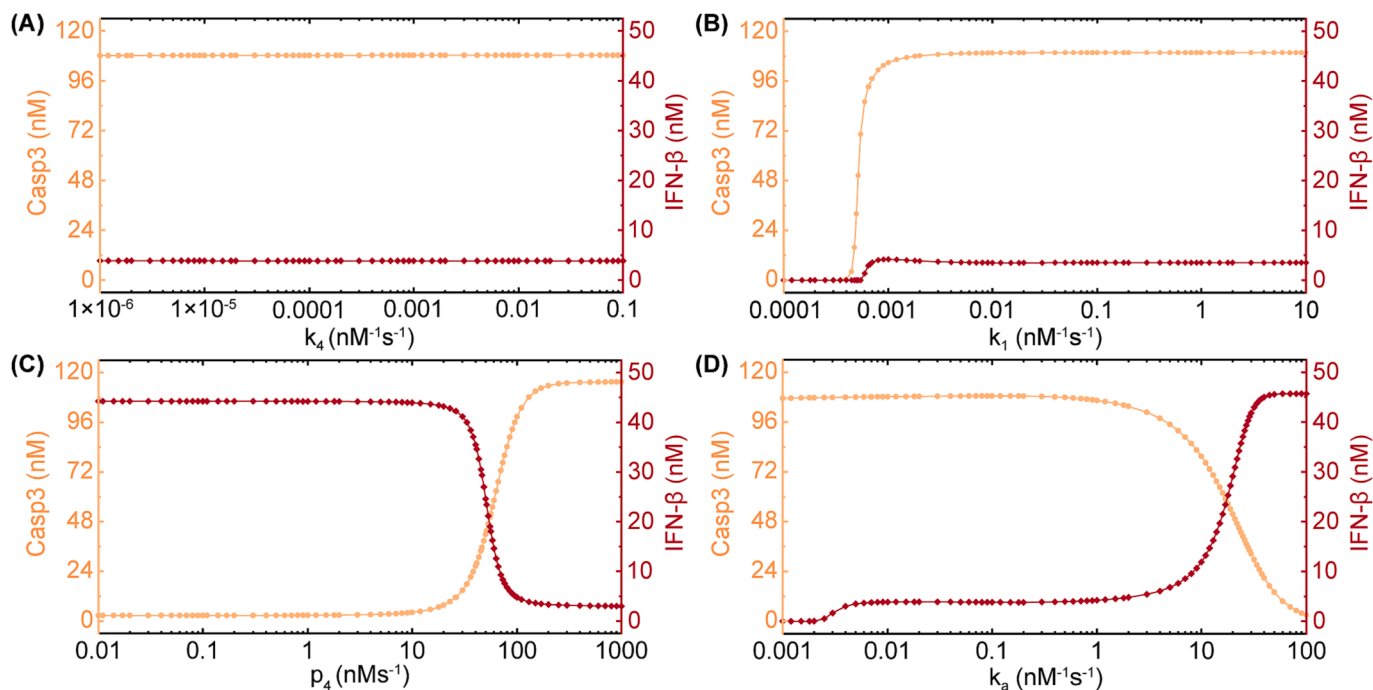


**Fig. 5.** Influence of different parameters on the amount of caspase 3 and IFN- $\beta$ . The physical meanings of the parameters  $k_4$ ,  $k_1$ ,  $p_4$ , and  $k_a$  are listed in Table S2 and explained in the main text.

inflammation.

Differently, the changes in production rate of Cyt c ( $p_4$ ) and dimerization rate constant of AcBax oligomers ( $k_a$ ) have significant influence on cell fate. As shown in Fig. 5C, when  $p_4$  is small, caspase 3 is in a low level and IFN- $\beta$  is in a high level; but with the increase of  $p_4$ , caspase 3 increases to a high level and IFN- $\beta$  drops to a low level. This means that with the increase of  $p_4$ , cell fate can switch from inflammation to apoptosis. In contrast to  $p_4$ , with the increase of  $k_a$ , cell fate can switch from apoptosis to inflammation (Fig. 5D).

**3.5. Influence of dimerization rate constant of AcBax oligomers ( $k_a$ ) on cell fate**

The result in Fig. 5D suggests that the parameter  $k_a$  can play a remarkable role in dictating cell fate decisions. For the purpose of illustration, we presented the details of the time series of all species in the last three modules for extremely small and big  $k_a$ .

Fig. 6 displays the results obtained when  $k_a$  equals 0.001. Compared with the results using standard parameter values (Fig. 3), the

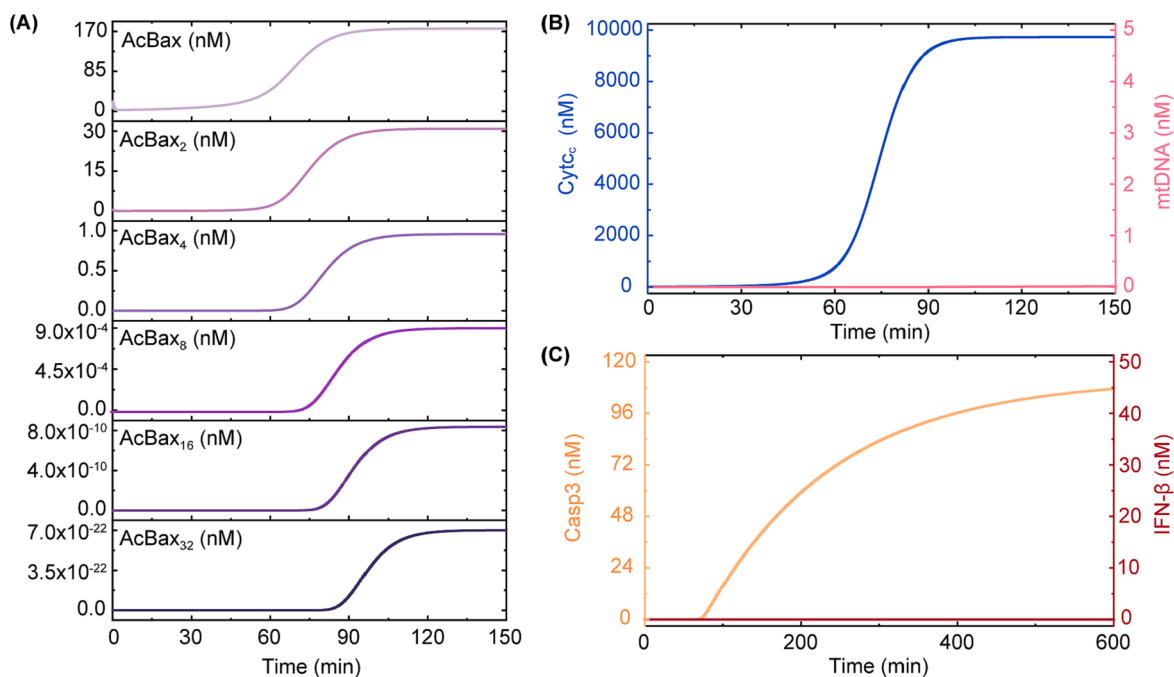


**Fig. 6.** The time courses of activated form of Bax (AcBax) and its  $n$ -order oligomers AcBax $_n$  (A), Cyt c and mtDNA in the cytosol (B), and caspase 3 and IFN- $\beta$  (C) at  $k_a = 0.001$ .  $k_a$ , dimerization rate constant of AcBax oligomers. Cyt c means the Cyt c in the cytosol.

concentrations of AcBax<sub>2</sub> and AcBax<sub>4</sub> do not change remarkably, whereas the concentrations of AcBax<sub>8</sub>, AcBax<sub>16</sub>, and AcBax<sub>32</sub> decrease very dramatically (Fig. 6A), which indicates that the constituents responsible for MIMP are very low. This leads to that almost all of the Cyt c is released into the cytoplasm, but mtDNA is not released (Fig. 6B). Thus, caspase 3 is sufficiently activated to cause apoptosis, while IFN- $\beta$  is not produced, without triggering inflammatory response (Fig. 6C).

However, the situation for  $k_a = 100$  looks different. Compared with the results shown in Fig. 3, the concentrations of AcBax<sub>2</sub>, AcBax<sub>4</sub>, and AcBax<sub>8</sub> are quite low, whereas the concentrations of AcBax<sub>16</sub> and AcBax<sub>32</sub> increase very strongly (Fig. 7A), which implies that the constituents responsible for MOMP are very low, and conversely, the constituents responsible for MIMP are strikingly high. This results in that only a small amount of Cyt c is released, but all of the mtDNA escape into the cytosol for activating IFN- $\beta$  (Fig. 7B). Therefore, caspase 3 is essentially silent, and IFN- $\beta$  is able to induce inflammatory response (Fig. 7C).

### 3.6. Other parameters that can regulate cell fate

Finally, we tested whether the parameters downstream of the release event (i.e.,  $k_5$ ,  $k_6$ ,  $k_{m1}$ ,  $k_{m2}$ , and  $k_{m3}$ ) can regulate cell fate. By the same analysis method as used in Section 3.5, we found that two out of the five parameters have strong influence on cell fate transition.

The situation for half-saturation constant of Cyt c-induced activation of caspase 3 ( $k_{m1}$ ) is similar to that for  $k_a$ . As depicted in Fig. 8A, when  $k_{m1}$  is small, caspase 3 is in a high level and IFN- $\beta$  is in a low level; but with the increase of  $k_{m1}$ , caspase 3 decreases to a low level and IFN- $\beta$  increases to a high level. This means that with the increase of  $k_{m1}$ , cell fate can switch from apoptosis without concomitant inflammation to inflammation.

The situation for half-saturation constant of caspase 3-dependent inhibition of IFN- $\beta$  production ( $k_{m2}$ ) is unique (Fig. 8B). For low values of  $k_{m2}$ , caspase 3 is in a high level and IFN- $\beta$  is in a low level.

Surprisingly, for high values of  $k_{m2}$ , although caspase 3 is kept in a high value, IFN- $\beta$  is also in a high level, indicating that apoptosis occurs with concomitant inflammation. This suggests that with the increase of  $k_{m2}$ , cell fate can be modified from apoptosis without concomitant inflammation to apoptosis with concomitant inflammation.

## 4. Discussion

Apoptosis and inflammation are two closely related processes (Hiller et al., 2003). Apoptosis is crucial for organismal development and homeostasis (Qi et al., 2018). In physiological conditions, inflammation is silenced during apoptosis (Vringer and Tait, 2023). Deregulated inflammatory responses are involved in a growing list of human diseases, including infection, cancers, and neurodegenerative and autoimmune diseases (Marchi et al., 2023; Morioka et al., 2022). Recently, multiple studies have established an intimate interplay between apoptosis and inflammation via Bax. Once activated, Bax forms dimers. The dimers assemble into small pores that execute MOMP, permitting the release of Cyt c. This process results in activation of caspase 3, and subsequent apoptosis (Große et al., 2016; Salvador-Gallego et al., 2016). The small pores can continue to grow into megapores that mediate MIMP, which causes mtDNA release, allowing it to activate cGAS-STING pathway and IFN- $\beta$  synthesis (McArthur et al., 2018; Riley et al., 2018). This process leads to inflammation, but in normal cells, caspase 3 prevents cGAS-STING signaling to preserve the non-inflammatory nature of apoptosis (Rongvaux et al., 2014; White et al., 2014). Despite these progresses, the detailed dynamical mechanism that link apoptosis and inflammation by mitochondrial membrane permeabilization remains obscure.

Due to the complexity of biological systems, mathematical modeling has become a powerful way for understanding their underlying mechanism (De Caluwé et al., 2019; Jia and Grima, 2020; Sun et al., 2015; Wang et al., 2022). In the present study, we refer to the small pores that execute MOMP as low-order oligomers and the megapores that mediate MIMP as high-order oligomers. We postulate that the assembly of

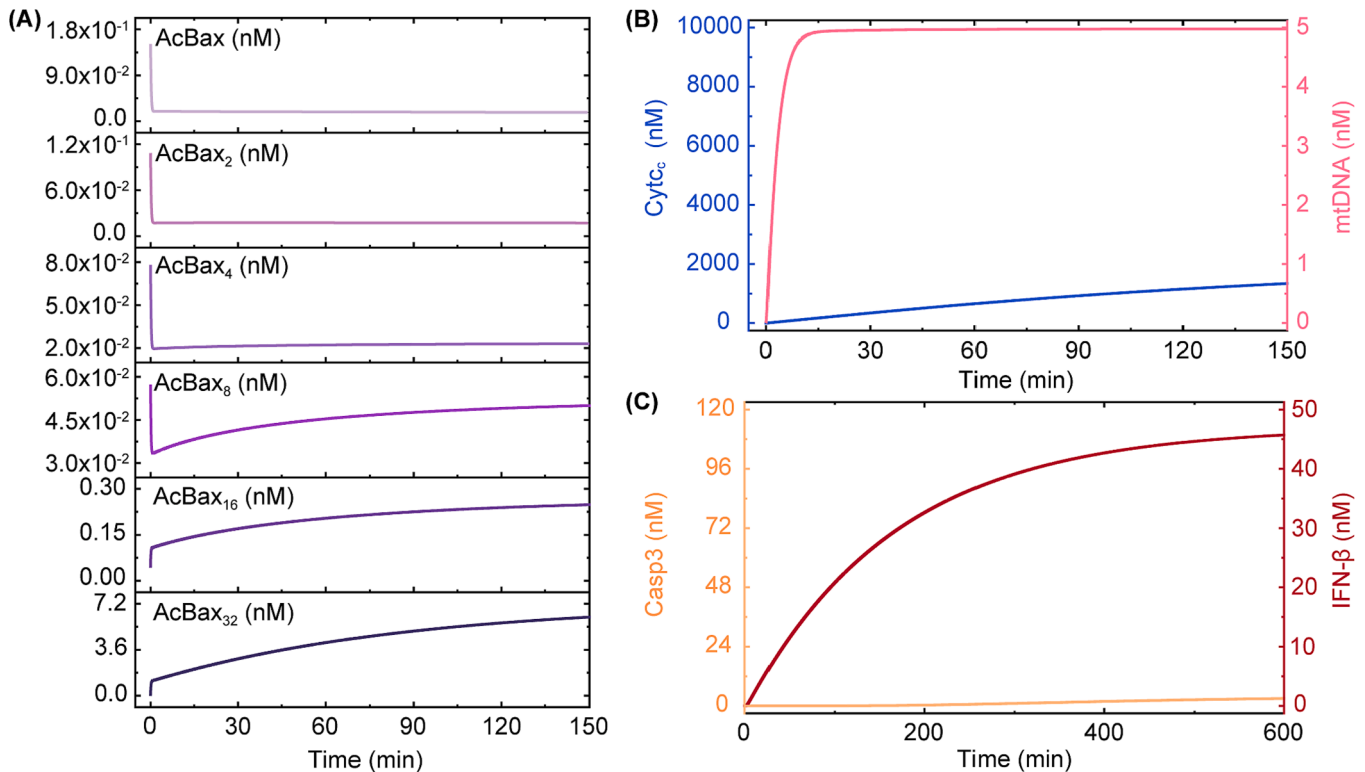


**Fig. 7.** The time courses of activated form of Bax (AcBax) and its n-order oligomers AcBax<sub>n</sub> (A), Cyt c and mtDNA in the cytosol (B), and caspase 3 and IFN- $\beta$  (C) at  $k_a = 100$ .  $k_a$ , dimerization rate constant of AcBax oligomers. Cyt c means the Cyt c in the cytosol.

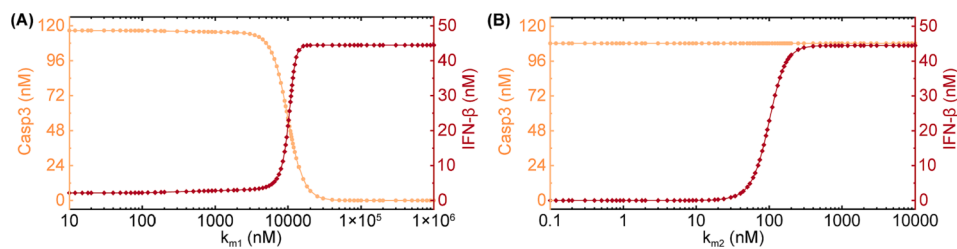


**Fig. 8.** Influence of  $k_{m1}$  and  $k_{m2}$  on the amount of caspase 3 and IFN- $\beta$ .  $k_{m1}$ , half-saturation constant of Cyt c-induced caspase 3 activation;  $k_{m2}$ , half-saturation constant of caspase 3-dependent inhibition of IFN- $\beta$  production.

different sizes of oligomers is a highly regulated process, which is vital for the release of Cyt c and mtDNA, and hence for the occurrence of apoptosis and inflammation. For the purpose of clarifying the dynamical mechanism linking apoptosis and inflammation, we construct an ODE model that consists of four modules: (1) interaction between members of Bcl-2 family, (2) assembling process of MOMP and MIMP, (3) Cyt c-induced caspase 3 activation, and (4) mtDNA-driven IFN- $\beta$  production. The model results can be summarized into two aspects.

On the one hand, although further validation of our model is required, the simulation results match the experimental observations well, lending credence to our hypothesis. The bifurcation analysis for the first two modules demonstrates that the occurrence of MOMP is bistable (Fig. 2), in line with the previous experimental and theoretical results (Chen et al., 2007; Sun et al., 2010; Yin et al., 2017). In addition, the time series analysis for the whole model shows that the time difference between Cyt c and mtDNA release is around 30 min (Fig. 3), which is roughly the same as the related experimental data (Cosentino and García-Sáez, 2018). Moreover, the robustness of this result is supported by parameter sensitivity analysis (Fig. 4).

On the other hand, some compelling predictions about cell fate regulation are obtained by testing the influence of 20 dynamical parameters (Table S2) on the amounts of caspase 3 and IFN- $\beta$ . Our results reveal that only four out of the 20 parameters, i.e.,  $p_4$ ,  $k_a$ ,  $k_{m1}$ , and  $k_{m2}$ , have regulatory roles in cell fate transition. Because of the positive correlation between Cyt c amount and caspase 3 activity as well as the negative correlation between caspase 3 activity and IFN- $\beta$  amount, it is easy to understand why the increase of production rate of Cyt c ( $p_4$ ) can switch the cell fate from inflammation to apoptosis (Fig. 5C). The results in Fig. 5D, Fig. 6, and Fig. 7 collectively suggest that the dimerization rate constant of AcBax oligomers ( $k_a$ ) modulates the amounts of low-order and high-order oligomers and thus the amounts of MOMP and MIMP, which significantly tune the relative release kinetics of Cyt c and mtDNA, thereby impacting downstream caspase 3 activity and IFN- $\beta$  production. This prediction is supported by a very recent report highlighting the important role of assembly rate of Bax in modulating the inflammatory outcome of apoptosis (Cosentino et al., 2022). As expected, the increase of half-saturation constant of Cyt c-induced caspase 3 activation ( $k_{m1}$ ) can switch the cell fate from apoptosis to inflammation (Fig. 8A), which is similar to the situation in  $k_a$ . Perhaps the most

striking finding is that high values of half-saturation constant of caspase 3-dependent inhibition of IFN- $\beta$  production ( $k_{m2}$ ) lead to apoptosis with concomitant inflammation (Fig. 8B), a phenomenon that is seldom observed in the experiments. These findings raise the interesting possibility that cell fate can be reversed or modified by manipulating the biological components or processes which are related to the four parameters.

Lastly, in view of the lack of precise information on some parameters and the existence of several assumptions in our model, the results obtained in the current work should be viewed as qualitative, rather than quantitative. However, these results begin to unravel the dynamical mechanism underpinning apoptosis and inflammation. Notably, we propose several potential strategies for cell fate decision, which may be clinically relevant and can be explored in future investigations. In conclusion, the present study is an important step towards understanding the intricate mechanism of mitochondrial membrane permeabilization in regulating cell fate.

#### CRedit authorship contribution statement

**Hong Qi:** Conceptualization, Methodology, Writing – original draft, Writing – review & editing. **Yu-Song Yin:** Methodology, Investigation, Writing – original draft. **Zhi-Yong Yin:** Conceptualization, Methodology. **Xiang Li:** Software, Visualization. **Jian-Wei Shuai:** Writing – review & editing, Supervision.

#### Declaration of Competing Interest

The authors declare that they have no known competing financial interests or personal relationships that could have appeared to influence the work reported in this paper.

#### Acknowledgments

This work is supported by the National Natural Science Foundation of China (Nos. 12275164, 12226317, and 12090052), STI2030-Major Projects 2021ZD0201900, and Wenzhou Key Laboratory of Biophysics (WIUCASSWWL22003).

## Appendix

**Table S1.** Equations of the model

#### Ordinary differential equations

$$\begin{aligned} d[Bax]dt &= j_1 - v_1 \\ d[Bim]dt &= j_2 - v_3 \\ d[Bad]dt &= j_3 - v_4 \\ d[Bcl-2]dt &= j_4 - v_2 - v_3 - v_4 \\ d[Bim Bcl-2]dt &= j_5 + v_3 \\ d[Bad Bcl-2]dt &= j_6 + v_4 \end{aligned}$$

$$\begin{aligned} d[AcBax_8]dt &= j_{11} + v_7 - 2 v_8 \\ d[AcBax_{16}]dt &= j_{12} + v_8 - 2 v_9 \\ d[AcBax_{32}]dt &= j_{13} + v_9 \\ d[Cytc_m]dt &= j_{14} - v_{10} \\ d[Cytc]dt &= j_{15} + v_{10} \cdot VIMS / VCyt \\ d[Casp3]dt &= j_{18} + v_{12} \end{aligned}$$

(continued on next page)

**Table S1. Equations of the model (continued)**

$d [Bcl-2:AcBax]dt = j_7 + v_2$	$d [mtDNA_m]dt = j_{16} - v_{11}$	
$d [AcBax]dt = j_8 + v_1 - v_2 - 2 v_5$	$d [mtDNA_c]dt = j_{17} + v_{11} \cdot V_{Mat} / V_{Cyt}$	
$d [AcBax_2]dt = j_9 + v_5 - 2 v_6$	$d [IFN-\beta]dt = j_{19} + v_{13}$	
$d [AcBax_4]dt = j_{10} + v_6 - 2 v_7$		
<b>Reaction rates</b>		
$v_1 = k_1 [Bim] \cdot [Bax]$	$v_6 = k_d \cdot [AcBax_2]^2 - k_d \cdot [AcBax_4]$	
$v_2 = k_2 \cdot [Bcl-2] \cdot [AcBax] - k_{-2} \cdot [Bcl-2:AcBax]$	$v_7 = k_d \cdot [AcBax_4]^2 - k_d \cdot [AcBax_8]$	
$v_3 = k_3 \cdot [Bim] \cdot [Bcl-2] - k_{-3} \cdot [Bim Bcl-2]$	$v_8 = k_d \cdot [AcBax_8]^2 - k_d \cdot [AcBax_{16}]$	
$v_4 = k_4 \cdot [Bad] \cdot [Bcl-2] - k_{-4} \cdot [Bad Bcl-2]$	$v_9 = k_d \cdot [AcBax_{16}]^2 - k_d \cdot [AcBax_{32}]$	
$v_5 = k_a \cdot [AcBax]^2 - k_d \cdot [AcBax_2]$		
$v_{10} = k_{rel1} [Cyt_c_m] \cdot ([AcBax_2] 2 + [AcBax_4] 4 + [AcBax_8])$		
$v_{11} = k_{rel2} [mtDNA_m] \cdot ([AcBax_8] 2 + [AcBax_{16}] 4 + [AcBax_{32}])$		
<b>Production-degradation rates</b>		
$j_1 = p_1 - u \cdot [Bax]$	$j_8 = -u \cdot [AcBax]$	$j_{15} = -u \cdot [Cyt_c]$
$j_2 = p_2 - u \cdot [Bim]$	$j_9 = -u \cdot [AcBax_2]$	$j_{16} = p_5 - u \cdot [mtDNA_m]$
$j_3 = p_3 - u \cdot [Bad]$	$j_{10} = -u \cdot [AcBax_4]$	$j_{17} = -u \cdot [mtDNA_c]$
$j_4 = p_3 - u \cdot [Bcl-2]$	$j_{11} = -u \cdot [AcBax_8]$	$j_{18} = -u \cdot [Casp3]$
$j_5 = -u \cdot [Bim Bcl-2]$	$j_{12} = -u \cdot [AcBax_{16}]$	$j_{19} = -u \cdot [IFN-\beta]$
$j_6 = -u \cdot [Bad Bcl-2]$	$j_{13} = -u \cdot [AcBax_{32}]$	
$j_7 = -u \cdot [Bcl-2:AcBax]$	$j_{14} = p_4 - u \cdot [Cyt_c_m]$	

**Table S2. List of standard parameters in the model**

Parameter	Description	Value (Unit)	Reference
$p_1$	Production rate of Bax	0.05 (nMs <sup>-1</sup> )	(1)
$p_2$	Production rates of Bim and Bad	0.0005 (nMs <sup>-1</sup> )	(1)
$p_3$	Production rate of Bcl-2	0.025 (nMs <sup>-1</sup> )	(1)
$p_4$	Production rate of Cyt c	130.0 (nMs <sup>-1</sup> )	(2)
$p_5$	Production rate of mtDNA	0.0072 (nMs <sup>-1</sup> )	(3,4)
$u$	Degradation rate constant of all species	0.0001 (s <sup>-1</sup> )	(2)
$k_1$	Bim-mediated activation rate constant of Bax	0.002 (nM <sup>-1</sup> s <sup>-1</sup> )	Assumed
$k_2$	Association rate constant of AcBax and Bcl-2	0.0002 (nM <sup>-1</sup> s <sup>-1</sup> )	(1)
$k_3$	Association rate constant of Bim and Bcl-2	0.0005 (nM <sup>-1</sup> s <sup>-1</sup> )	(1)
$k_4$	Association rate constant of Bad and Bcl-2	0.00005 (nM <sup>-1</sup> s <sup>-1</sup> )	(1)
$k_{-}$	Dissociation rate constant of complexes	0.001 (s <sup>-1</sup> )	(1)
$k_a$	Dimerization rate constant of AcBax <sub>n</sub>	0.01 (nM <sup>-1</sup> s <sup>-1</sup> )	Assumed
$k_d$	Dissociation rate constant of AcBax <sub>2n</sub>	1.0 (s <sup>-1</sup> )	(5)
$k_{rel1}$	Release rate constant of Cyt c	0.0001 (nM <sup>-1</sup> s <sup>-1</sup> )	Assumed
$k_{rel2}$	Release rate constant of mtDNA	0.001 (nM <sup>-1</sup> s <sup>-1</sup> )	10 $k_{rel1}$
$k_5$	Activation rate constant of caspase 3	0.012 (nMs <sup>-1</sup> )	(2)
$km_1$	Half-saturation constant of Cyt c-induced caspase 3 activation	5000.0 (nM)	Assumed
$k_6$	Production rate constant of IFN-β	0.005 (nMs <sup>-1</sup> )	Assumed
$km_2$	Half-saturation constant of caspase 3-dependent inhibition of IFN-β production	50.0 (nM)	Assumed
$km_3$	Half-saturation constant of mtDNA-dependent activation of IFN-β production	2.5 (nM)	Assumed
$V_{IMS}$	Volume of mitochondrial intermembrane space	30.0 (μm <sup>3</sup> )	(2)
$V_{Mat}$	Volume of mitochondrial matrix	270.0 (μm <sup>3</sup> )	(2)
$V_{Cyt}$	Volume of cytosolic compartment	3890.0 (μm <sup>3</sup> )	(2)

**References**

- Yin Z., Qi H., Liu L., Jin Z., 2017. The optimal regulation mode of Bcl-2 apoptotic switch revealed by bistability analysis. *BioSystems*. 162, 44–52.
- Qi H., Li X., Jin Z., Simmen T., Shuai J., 2020. The oscillation amplitude, not the frequency of cytosolic calcium, regulates apoptosis induction. *iScience*. 23, 101671.
- Satoh M., Kuroiwa T., 1991. Organization of multiple nucleoids and DNA molecules in mitochondria of a human cell. *Exp. Cell Res.* 196, 137–40.
- Frahm T., Mohamed S. A., Bruse P., Gemünd C., Oehmichen M., Meissner C., 2005. Lack of age-related increase of mitochondrial DNA amount in brain, skeletal muscle and human heart. *Mech. Ageing Dev.* 126, 1192–200.
- Kueh H. Y., Zhu Y., Shi J., 2016. A simplified Bcl-2 network model reveals quantitative determinants of cell-to-cell variation in sensitivity to anti-mitotic chemotherapeutics. *Sci. Rep.* 6, 1–13.

**References**

Bedoui, S., Herold, M.J., Strasser, A., 2020. Emerging connectivity of programmed cell death pathways and its physiological implications. *Nat. Rev. Mol. Cell Biol.* 21 (11), 678–695.

Chen, C., Cui, J., Lu, H., Wang, R., Zhang, S., Shen, P., 2007. Modeling of the role of a Bax-activation switch in the mitochondrial apoptosis decision. *Biophys. J.* 92 (12), 4304–4315.

Albeck, J.G., Burke, J.M., Spencer, S.L., Lauffenburger, D.A., Sorger, P.K., Levchenko, A., 2008. Modeling a snap-action, variable-delay switch controlling extrinsic cell death. *PLoS Biol.* 6 (12).

- Cosentino, K., García-Sáez, A.J., 2018. MIM through MOM: the awakening of Bax and Bak pores. *EMBO J.* 37, e100340.
- Cosentino, K., Hertlein, V., Jenner, A., Dellmann, T., Gokjovic, M., Peña-Blanco, A., Dadsena, S., Wajngarten, N., Danial, J.S.H., Thevathasan, J.V., Mund, M., Ries, J., García-Sáez, A.J., 2022. The interplay between BAX and BAK tunes apoptotic pore growth to control mitochondrial-DNA-mediated inflammation. *Mol. Cell* 82 (5), 933–949.e9.
- Cui, J., Chen, C., Lu, H., Sun, T., Shen, P., Hatakeyama, M., 2008. Two independent positive feedbacks and bistability in the Bcl-2 apoptotic switch. *PLoS One* 3 (1), e1469.
- Czabotar, P.E., Lessene, G., Strasser, A., Adams, J.M., 2014. Control of apoptosis by the BCL-2 protein family: implications for physiology and therapy. *Nat. Rev. Mol. Cell Biol.* 15 (1), 49–63.
- De Caluwé, J., Tosenberger, A., Gonze, D., Dupont, G., 2019. Signalling-modulated gene regulatory networks in early mammalian development. *J. Theor. Biol.* 463, 56–66.
- Fox, R., Aubert, M., 2008. Flow cytometric detection of activated caspase-3. *Methods Mol. Biol.* 414, 47–56.
- Frahm, T., Mohamed, S.A., Bruse, P., Gemünd, C., Oehmichen, M., Meissner, C., 2005. Lack of age-related increase of mitochondrial DNA amount in brain, skeletal muscle and human heart. *Mech. Ageing Dev.* 126 (11), 1192–1200.
- Frank, A.S., Larripa, K., Ryu, H., Snodgrass, R.G., Röblitz, S., 2021. Bifurcation and sensitivity analysis reveal key drivers of multistability in a model of macrophage polarization. *J. Theor. Biol.* 509.
- Galluzzi, L., Vanpouille-Box, C., 2018. BAX and BAK at the gates of innate immunity. *Trends Cell Biol.* 28 (5), 343–345.
- Green, D., Levine, B., 2014. To be or not to be? How selective autophagy and cell death govern cell fate. *Cell* 157 (1), 65–75.
- Große, L., Wurm, C.A., Brüser, C., Neumann, D., Jans, D.C., Jakobs, S., 2016. Bax assembles into large ring-like structures remodeling the mitochondrial outer membrane in apoptosis. *EMBO J.* 35, 402–413.
- Gutiérrez, T., Qi, H., Yap, C.M., Tahbaz, N., Milburn, A.L., Lucchinetti, E., Lou, P.-H., Zaugg, M., LaPointe, P.G., Mercier, P., Overduin, M., Bischof, H., Burgstaller, S., Malli, R., Ballanyi, K., Shuai, J., Simmen, T., 2020. The ER chaperone calnexin controls mitochondrial positioning and respiration. *Sci. Signal.* 13, eaax6660.
- Hantusch, A., Rehm, M., Brunner, T., 2018. Counting on death-quantitative aspects of Bcl-2 family regulation. *FEBS J.* 285 (22), 4124–4138.
- Hiller, S., Kohl, A., Fiorito, F., Herrmann, T., Wider, G., Tschopp, J., Grütter, M.G., Wüthrich, K., 2003. NMR structure of the apoptosis- and inflammation-related NALP1 pyrin domain. *Structure* 11 (10), 1199–1205.
- Huber, H.J., Duessmann, H., Wenus, J., Kilbride, S.M., Prehn, J.H.M., 2011. Mathematical modelling of the mitochondrial apoptosis pathway. *BBA-Mol. Cell Res.* 1813 (4), 608–615.
- Jia, C., Grima, R., 2020. Small protein number effects in stochastic models of autoregulated bursty gene expression. *J. Chem. Phys.* 152 (8).
- Kueh, H.Y., Zhu, Y., Shi, J., 2016. A simplified Bcl-2 network model reveals quantitative determinants of cell-to-cell variation in sensitivity to anti-mitotic chemotherapeutics. *Sci. Rep.* 6, 1–13.
- Lee, J.K., Lu, S., Madhukar, A., Linden, R., 2010. Real-time dynamics of Ca<sup>2+</sup>, caspase-3/7, and morphological changes in retinal ganglion cell apoptosis under elevated pressure. *PLoS One* 5 (10).
- Marchi, S., Guilbaud, E., Tait, S.W.G., Yamazaki, T., Galluzzi, L., 2023. Mitochondrial control of inflammation. *Nat. Rev. Immunol.* 23 (3), 159–173.
- McArthur, K., Whitehead, W.L., Hedderston, M.J., Li, L., Padman, S.B., Oorschot, V., Geoghegan, N.D., Chappaz, S., Davidson, S., San Chin, H., Lane, R.M., Dramicanin, M., Saunders, T.L., Sugiana, C., Lessene, R., Osellame, L.D., Chew, T.-L., Dewson, G., Lazarou, M., Ramm, G., Lessene, G., Ryan, M.T., Rogers, K.L., van Delft, M.F., Kile, B.T., 2018. BAK/BAX macropores facilitate mitochondrial herniation and mtDNA efflux during apoptosis. *Science* 359, eaao6047.
- Morioka, S., Kajioka, D., Yamaoka, Y., Ellison, R.M., Tufan, T., Werkman, I.L., Tanaka, S., Barron, B., Ito, S.T., Kucenas, S., Okusa, M.D., Ravichandran, K.S., 2022. Chimeric efferoctytic receptors improve apoptotic cell clearance and alleviate inflammation. *Cell* 185 (26), 4887–4903.e17.
- Mu, D., Qin, H., Jiao, M., Hua, S., Sun, T., 2021. Modeling the neuro-protection of theaflavin acid from black tea and its synergy with nimodipine via mitochondria apoptotic pathway. *J. Zhejiang Univ. Sci. B* 22 (2), 123–135.
- Ning, X., Wang, Y., Jing, M., Sha, M., Lv, M., Gao, P., Zhang, R., Huang, X., Feng, J.-M., Jiang, Z., 2019. Apoptotic caspases suppress type I interferon production via the cleavage of cGAS, MAVS, and IRF3. *Mol. Cell* 74 (1), 19–31.e7.
- Ow, Y.-L., Green, D.R., Hao, Z., Mak, T.W., 2008. Cytochrome c: functions beyond respiration. *Nat. Rev. Mol. Cell Biol.* 9 (7), 532–542.
- Pfanner, N., Warscheid, B., Wiedemann, N., 2019. Mitochondrial proteins: from biogenesis to functional networks. *Nat. Rev. Mol. Cell Biol.* 20 (5), 267–284.
- Qi, H., Jiang, Y.u., Yin, Z., Jiang, K.e., Li, L., Shuai, J., 2018. Optimal pathways for the assembly of the Apaf-1-cytochrome c complex into apoptosome. *Phys. Chem. Chem. Phys.* 20 (3), 1964–1973.
- Qi, H., Li, X., Jin, Z., Simmen, T., Shuai, J., 2020a. The oscillation amplitude, not the frequency of cytosolic calcium, regulates apoptosis induction. *iScience* 23 (11).
- Qi, H., Xu, G., Peng, X.-L., Li, X., Shuai, J., Xu, R., 2020b. Roles of four feedback loops in mitochondrial permeability transition pore opening induced by Ca<sup>2+</sup> and reactive oxygen species. *Phys. Rev. E* 102, 062422.
- Qi, H., Li, Z.-C., Wang, S.-M., Wu, L., Xu, F., Liu, Z.-L., Li, X., Wang, J.-Z., 2021. Tristability in mitochondrial permeability transition pore opening. *Chaos* 31 (12).
- Riley, J.S., Quarato, G., Cloix, C., Lopez, J., O'Prey, J., Pearson, M., Chapman, J., Sesaki, H., Carlin, L.M., Passos, J.F., 2018. Mitochondrial inner membrane permeabilisation enables mtDNA release during apoptosis. *EMBO J.* 37, e99238.
- Rongvaux, A., Jackson, R., Harman, C.D., Li, T., West, A.P., de Zoete, M., Wu, Y., Yordy, B., Lakhani, S., Kuan, C.-Y., Taniguchi, T., Shadel, G., Chen, Z., Iwasaki, A., Flavell, R., 2014. Apoptotic caspases prevent the induction of type I interferons by mitochondrial DNA. *Cell* 159 (7), 1563–1577.
- Salvador-Gallego, R., Mund, M., Cosentino, K., Schneider, J., Unsay, J., Schraermeyer, U., Engelhardt, J., Ries, J., García-Sáez, A.J., 2016. Bax assembly into rings and arcs in apoptotic mitochondria is linked to membrane pores. *EMBO J.* 35 (4), 389–401.
- Sarosiek, K., Chi, X., Bachman, J., Sims, J., Montero, J., Patel, L., Flanagan, A., Andrews, D., Sorger, P., Letai, A., 2013. BID preferentially activates BAK while BIM preferentially activates BAX, affecting chemotherapy response. *Mol. Cell* 51 (6), 751–765.
- Satoh, M., Kuroiwa, T., 1991. Organization of multiple nucleoids and DNA molecules in mitochondria of a human cell. *Exp. Cell Res.* 196, 137–140.
- Singh, R., Letai, A., Sarosiek, K., 2019. Regulation of apoptosis in health and disease: the balancing act of BCL-2 family proteins. *Nat. Rev. Mol. Cell Biol.* 20 (3), 175–193.
- Subburaj, Y., Cosentino, K., Axmann, M., Pedrueza-Villalmanzo, E., Herrmann, E., Bleicken, S., Spatz, J., García-Sáez, A.J., 2015. Bax monomers form dimer units in the membrane that further self-assemble into multiple oligomeric species. *Nat. Commun.* 6, 1–11.
- Sun, T., Lin, X., Wei, Y., Xu, Y., Shen, P., 2010. Evaluating bistability of Bax activation switch. *FEBS Lett.* 584, 954–960.
- Sun, X., Zheng, X., Zhang, J., Zhou, T., Yan, G., Zhu, W., 2015. Mathematical modeling reveals a critical role for cyclin D1 dynamics in phenotype switching during glioma differentiation. *FEBS Lett.* 589, 2304–2311.
- Vringer, E., Tait, S.W.G., 2023. Mitochondria and cell death-associated inflammation. *Cell Death Differ.* 30 (2), 304–312.
- Wang, D., Ghosh, D., Islam, S.M.T., Moorman, C.D., Thomason, A.E., Wilkinson, D.S., Mannie, M.D., 2016. IFN- $\beta$  facilitates neuroantigen-dependent induction of CD25<sup>+</sup> FOXP3<sup>+</sup> regulatory T cells that suppress experimental autoimmune encephalomyelitis. *J. Immunol.* 197 (8), 2992–3007.
- Wang, P., Guan, D.i., Zhang, X.-P., Liu, F., Wang, W., 2019. Modeling the regulation of p53 activation by HIF-1 upon hypoxia. *FEBS Lett.* 593 (18), 2596–2611.
- Wang, H.-Y., Zhang, X.-P., Wang, W., 2022. Regulation of epithelial-to-mesenchymal transition in hypoxia by the HIF-1 $\alpha$  network. *FEBS Lett.* 596 (3), 338–349.
- White, J. M., McArthur, K., Metcalf, D., Lane, M. R., Cambier, C. J., Herold, M. J., van Delft, M. F., Bedoui, S., Lessene, G., Ritchie, M. E., Huang, D. C. S., Kile, B. T., 2014. Apoptotic caspases suppress mtDNA-induced STING-mediated type I IFN production. *Cell* 159, 1549–1562.
- Yin, Z., Qi, H., f. L., Jin, Z., 2017. The optimal regulation mode of Bcl-2 apoptotic switch revealed by bistability analysis. *Biosystems* 162, 44–52.
- Youle, J.R., 2019. Mitochondria-striking a balance between host and endosymbiont. *Science* 365, eaaw9855.
- Youle, R.J., Strasser, A., 2008. The BCL-2 protein family: Opposing activities that mediate cell death. *Nat. Rev. Mol. Cell Biol.* 9 (1), 47–59.
- Zhang, X.-P., Liu, F., Wang, W., 2011. Two-phase dynamics of p53 in the DNA damage response. *Proc. Natl. Acad. Sci. USA* 108 (22), 8990–8995.